NASA Technical Memorandum 79112

SOME EFFECTS OF CYCLIC INDUCED DEFORMATION IN ROCKET THRUST CHAMBERS

N. P. Hannum, R. J. Quentmeyer, and H. J. Kasper
Lewis Research Center
Cleveland, Ohio

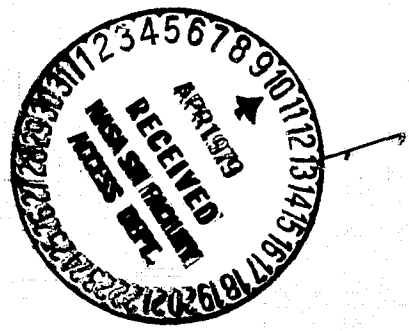

TECHNICAL PAPER to be presented at the
Conference on Advanced Technology for Future Space Systems
sponsored by the American Institute of Aeronautics and Astronautics
Hampton, Virginia, May 8-11, 1979

SOME EFFECTS OF CYCLIC INDUCED DEFORMATION IN ROCKET THRUST CHAMBERS

N. P. Hannum, R. J. Quentmeyer, and H. J. Kasper
National Aeronautics and Space Administration
Lewis Research Center
Cleveland, Ohio

Abstract

A test program to investigate the deformation process observed in the hot gas wall of rocket thrust chambers was conducted using three different liner materials. Five thrust chambers were cycled to failure using hydrogen and oxygen as propellants at a chamber pressure of 4.14 MN/m^2 (600 psia). The deformation was observed nondestructively at midlife points and destructively after failure occurred. The cyclic life results are presented with an accompanying discussion about the types of failure encountered. Data indicating the deformation of the thrust chamber liner as cycles are accumulated are presented for each of the test thrust chambers.

Introduction

The requirement for reusability of high-chamber-pressure, regeneratively cooled, rocket thrust chambers in the near future has precipitated experimental and analytical thermal fatigue studies related to thrust chamber life. The heat flux associated with the high chamber pressures (13.8 to 20.7 MN/m^2 (2000 to 3000 psia)) used in such high-performance engines cannot be accomodated by low-thermal-conductivity materials with wall thicknesses necessary for the pressure loads. Therefore, high-thermal-conductivity materials, such as copper or copper alloys, must be used for the thrust chamber walls. The expected design life for these future reusable thrust chambers is from 100 to 300 cycles. The work reported herein was not intended to demonstrate a particular life goal but rather to produce several thermal fatigue failures in rocket thrust chambers for the purpose of enhancing our knowledge of such failures and improving the present capabilities in thermal fatigue analysis and life prediction.

In 1972, low-cycle thermal fatigue tests were conducted by the U.S. Air Force on rocket combustion chambers that had been designed and fabricated by Rocketdyne.[1,2] These tests were conducted at a chamber pressure of 5.2 MN/m^2 (750 psia). Experimentally obtained fatigue life was compared without success with the analytical predictions of life for two zirconium-copper alloy thrust chambers. The NASA Marshall Space Flight Center later acquired more of these chambers and continued the work. The life analysis for these tests is reported in Ref. 3.

In this previous work, the life limiting failure mechanism was thought to be low cycle thermal fatigue. The controlling parameters were, therefore, the temperature difference between the hot gas side wall and the backside, the coefficient of thermal expansion for the liner material, and the geometry of the thrust chamber liner. The fatigue life was related to the strain range which occurs in the liner during a thermal cycle. The finite element models used to compute strain range assumed that the geometry remained fixed throughout the life of the thrust chamber.

In 1973 work began at the Lewis Research Center to systematically investigate the problem of thrust chamber life. The approach was to significantly increase the data base of thrust chamber fatigue failures using cyclic testing under controlled conditions and with a test procedure designed specifically to study thrust chamber life. Inexpensive cylinders with plug nozzles were used to evaluate various thrust chamber liner materials over a range of hot gas wall temperature. These experimental life data were correlated both with the hot gas wall temperature and the temperature difference between the hot gas surface and the outside surface for each material tested.[4] Finite element analysis was conducted to compute strain range. Attempts were made to predict life assuming a low cycle thermal fatigue failure mechanism and using life data from uniaxial isothermal fatigue tests as reference. This life prediction procedure was generally not successful for either the cylindrical thrust chambers of Ref. 4 or the contoured thrust chambers of Ref. 5. The analysis was used, however, to indicate that reducing the stiffness of the outer wall structure (closeout) of the thrust chamber could reduce the strain range. Contoured thrust chambers were fabricated and tested to experimentally investigate this predicted trend. The closeout stiffness was reduced by replacing most of the thick electroformed closeout with a fiberglass wrap. An increase in life was observed.[6] Life can also be increased by decreasing the hot gas wall temperature as reported in Ref. 4 and as shown by various analytical studies. Life improvement was accomplished experimentally by applying a coating to the hot gas surface of cylindrical thrust chambers to reduce the temperature of the metal thrust chamber liner.[7]

Although some success was achieved in predicting trends, a priori life prediction was still not possible apparently because the failure mechanism was not properly described by the low cycle thermal fatigue model assumed in the analysis.

A more detailed description of the behavior of the thrust chamber hot gas wall in the vicinity of the failure site was needed to contribute to understanding of the failure mechanism. In response to this need five thrust chambers were fabricated from three different liner materials and tested at the Lewis Research Center. The objectives of the experimental investigation were to (1) obtain hot gas wall deformation data throughout the life span of rocket thrust chambers, and (2) obtain cyclic life and hot gas wall deformation data for different liner materials. In the course of this investigation nondestructive methods were used for locating potential failure sites early in the life of a thrust chamber and for making periodic measurements of the deformation.

The thrust chambers used in the investigation had a throat diameter of 6.60 cm (2.60 in.) and were operated at a chamber pressure of 4.14 MN/m^2 (600 psia). The propellants were liquid oxygen and gaseous hydrogen. The chambers were cooled with a separate flow of liquid hydrogen. The thrust cham-

AIAA Paper No. 79-0911

bers were made using fabrication methods that are typical for high pressure, high performance rocket engines such as Space Shuttle Main Engine. Coolant passages were milled into a high thermal conductivity liner. Nickel was then electrodeposited onto the liner to close-out the coolant channel and form the outer structural jacket.

Apparatus

Test Facility

The investigation was conducted at the Lewis Research Center rocket engine test facility. This is a 222 410-newton (50 000-lbf), sea-level rocket test stand equipped with an exhaust-gas muffler and scrubber. The facility used pressurized propellant-storage tanks to supply the propellants to the combustor. Propellants for combustion were liquid oxygen and ambient temperature gaseous hydrogen. Liquid hydrogen was used as the thrust chamber coolant. The separate coolant flow circuit was used to allow coolant flow to be independent of engine propellant flow. The spent hydrogen coolant was disposed of through a burn stack.

Injectors

With the injectors used in this investigation, the fuel (gaseous hydrogen) was injected through a porous Rigimesh face plate. The oxidant was injected through 85 showerhead tubes distributed evenly over the injector face. The energy release efficiency, which was determined from short duration tests with heat sink thrust chambers, was 97.5% with all data within a scatter band of ±0.5%. The performance procedure used to compute injector efficiency is outlined in Ref. 8.

During the performance testing with the heat-sink thrust chambers, tests were made with high-response piezoelectric pressure transducers installed on the thrust chamber to measure combustion chamber pressure oscillations and thereby to ascertain whether combustion instability was present. No instability was found.

Combustion Chambers

The details of the thrust chambers used in the fatigue life investigation are shown in Fig. 1. The completed chamber is shown in Fig. 1(a). The chambers, which had a contraction ratio of 3.70, were 38.1 cm (15 in.) in length overall with the throat located 25.4 cm (10 in.) from the injector face. The throat was 6.60 cm (2.6 in.) in diameter, and the nozzle exit was 13.2 cm (5.2 in.) in diameter. The chamber liners were made of copper or a copper alloy and had coolant passages machined into the outer surface. After machining, the coolant passages were temporarily filled with a wax, and a layer of nickel was electrodeposited onto the outer surface to close out the coolant channels and form the outer structural jacket. The coolant passage cross section thus formed is shown in Fig. 1(b), which is a section through the throat plane of the chamber. The coolant passage dimensions were selected to provide a hot-gas-side wall temperature of 811 K (1460° R) in the throat for the operating conditions of 4.14 MN/m^2 (600-psia) chamber pressure and 0.91-kg/sec (2.0-lb/sec) coolant flow rate. Much lower design temperatures were selected for other areas of the chamber to insure that the throat would be the region of highest strain. Spring loaded thermocouples were used to measure rib temperature. The location of these thermocouples is shown in Fig. 1(b). All chambers used in the testing were designed with the same coolant passage dimensions at the throat section. After electroforming, the wax was melted out of the coolant passages, the manifolds welded on, and the instrumentation attached.

A different closeout procedure was used for the two OFHC liners reported in the present work. Instead of the relatively thick (0.485 cm, 0.191 in.) nickel closeout, the OFHC liners were closed out with a two-part, low stiffness structure composed of a thin electroformed copper closeout and a fiberglass overwrap for hoop strength. All other dimensions and details were the same as those described above. The specific details of these low stiffness OFHC copper chambers are further described in Ref. 6.

Combustion Chamber Liner Materials

The liner materials were OFHC copper or copper alloys. One alloy was copper with 0.15% zirconium available from AMAX Corporation as Amzirc. The other alloy was copper with 0.45% zirconium, 3% silver available from Rocketdyne as Narloy-Z. The OFHC copper liner material was in the as forged condition. The Narloy-Z and Amzirc liners were solution annealed and aged. There were two OFHC copper liners, two Narloy-Z liners, and one heat treated Amzirc liner tested in this program. The serial number, liner material and material condition of the chambers are listed in Table I.

Procedure

With the test cycle selected for this program the maximum temperature difference between the hot gas wall and the chamber outside surface occurred during the fast start transient. The combustion chamber reached full chamber pressure in 0.05 to 0.06 sec, and the maximum temperature difference across the wall was equal to approximately 130% of the steady-state value. Once the test firing was well beyond the time when the maximum temperature difference had occurred, which was approximately 0.03 sec after start, the chamber was shut down. This gave a rated thrust duration of about 0.85 sec. The liquid hydrogen coolant flow was continued during a 1.4-sec shutdown period, which was enough time to cool all parts of the chamber to the original temperature conditions. This gave a total cycle duration of 2.3 sec. Then the test cycle was repeated until failure occurred. The propellant storage capability of the facility permitted as many as 125 cycles in a single firing series.

The test cycle was programmed into a solid-state timer that was accurate and repeatable to within ±0.001 sec. Fuel and oxidizer flows were controlled by fixed-position valves and propellant tank pressures. Coolant flow was controlled by a cavitating venturi. Coolant inlet pressure was controlled by coolant tank pressure, and the coolant exit pressure was kept constant by a closed-loop controller modulating a backpressure valve. Control room operation of the test included monitoring of

the test hardward by means of three closed-circuit television cameras and one microphone.

The output of the microphone and one television camera were recorded on magnetic tape for later playback. The microphone was used to determine the time of the fatigue failure. During the cooldown phase of a cycle, any coolant leak through a crack in the wall of the combustion chamber could be heard clearly. In most cases it was possible to recognize a failure and to stop the cyclic testing within two cycles of the failure. During play back of the audio tape, the exact cycle when failure occurred could be precisely determined.

After every series of test cycles, gaseous helium was introduced into the coolant channels remotely and trapped there under pressure. The presence of a pressure decay would indicate the presence of a crack through the thrust chamber liner. If a crack was indicated the facility was shut down and the crack was located by direct observation. Methods for measuring the hot gas wall deformation both on the test stand and in an inspection facility were developed and will be described in RESULTS AND DISCUSSION. These methods were used both at intermediate life points and for post failure data.

Results and Discussion

Experimental results are presented from testing five rocket thrust chambers. Tests consisted of repeated firings of each of the rocket thrust chambers until a crack occurred in the liner wall allowing coolant to leak into the combustion chamber. The cyclic life results will be presented with an accompanying discussion about the types of failures encountered in the present work. Data indicating the deformation of the thrust chamber liner as cycles are accumulated are presented for each of the test thrust chambers.

Test Conditions

The nominal steady state combustion chamber pressure was 4.14 MN/m^2 (600 psia) and the nominal coolant flow rate was 0.91 kg/sec (2.0 lb/sec). Care was taken to insure that the combustion propellant and coolant flow rates and pressures were nearly the same for each cycle of a test series. The steady state oxidant-fuel ratio was nominally 6.0 and was held within a range of approximately ±0.15 for all tests. Combustion chamber pressure did not vary more than ±3% from the nominal value. Coolant flow rate did not vary more than ±2% from the nominal value. Experimental data reported in Ref. 5 have shown that a ±2% variation in coolant flow rate is equivalent to ±11 K (±20° R) variation in rib temperature. Typical rib temperature data for a single cycle are presented in Fig. 2. The data presented are typical of all chambers tested in terms of transient response and the range of data between the four thermocouples. The difference in temperature between the hottest and the coldest circumferential locations was approximately 69 K (125° R) at the end of the transient and less toward the end of the firing. The rise time for the chamber pressure transient was approximately 50 msec. The rib temperature transient occurred in approximately 0.4 sec. Also shown in Fig. 2 are typical chamber outer surface temperature data as a function of time for one cycle. It can be seen that this parameter does not come to steady state during the short duration cycle.

Cycles to Failure

For this investigation, a fatigue failure was defined as a crack through the hot gas wall that permitted audible detection of a coolant leak into the combustion chamber during the nonfiring portion of the cycle. Cracks of approximately 1000 μm (0.039 in.) in length were the minimum size detected by this method. Most tests were manually aborted within one or two cycles after it was suspected that a failure had occurred. The coolant passages were then pressure checked to determine the number and location(s) of the failures.

The experimentally determined cyclic life for each of the five chambers tested in this program is shown in Table I. One of the two Narloy-Z chambers (S/N 140) failed after 301 cycles. The second Narloy-Z chamber (S/N 150) failed after 154 cycles. After 250 cycles, inspection of the heat treated Amzirc chamber, S/N 82, revealed three very small pin holes and one small crack. Therefore, there is some uncertainty about the exact cycle in which failure occurred. The two OFHC copper chambers (S/N 74 and 75) failed at 193 and 202 cycles, respectively.

Description of Failure Sites

The failures are generally characterized by a thinning and bulging of the hot gas wall. Also, there was a roughening of the hot gas side wall, especially in the throat region of the thrust chamber. Figure 3(a) is a view of the hot gas side wall showing the general surface roughening for OFHC copper chamber S/N 74. A 3.5 cm (1.4 in.) long crack at the center line of a coolant channel can also be seen. The roughening was more severe with the OFHC copper than with the Narloy-Z and heat treated Amzirc. The roughening was more severe in the throat region where the temperature was higher than at other locations in the combustion chamber.

A cross section, at the throat, of an entire thrust chamber is shown in Fig. 3(b). This is the OFHC copper chamber S/N 74 which had the low stiffness closeout described in the Apparatus section. The fiberglass portion of the closeout has been removed. It can be seen in Fig. 3(b) that the deformation is not the same in each of the 60 coolant channels. The circumferential location of the most severe deformation seems to be random, that is, not related to injector patterns, cooling manifolds, or fabrication anomalies that are within the drawing specifications.

Cross section views of the failure sites for two different materials are shown in Fig. 4. The failed coolant channel is characterized by a "dog house" shape and a bulge of the hot gas wall toward the centerline of the thrust chamber. Conservation of the wall material was assumed since no hot gas surface melt or erosion was observed. The hot gas wall must thin, therefore, to accommodate the bulge. Because of the progressive thinning, the bulge on the hot gas wall tends to form two bumps per cooling channel. It can be seen in Fig. 4(a) that the bulging and thinning that occurred with the OFHC copper material was much greater than with the

Narloy-Z (Fig. 4(b)). The failure sites for the other thrust chambers not shown also had the "dog house" shape. Although all materials deformed similarly, an important difference is evident between the two failure sites shown in Fig. 4. In addition to the thinning of the hot gas wall, a necking of the material in a small region on each side of the failure site occurred with the OFHC copper. This is a typical appearance of a tensile failure with a ductile material. Tensile failures were observed in Ref. 4 for OFHC copper, heat treated Amzirc, and Narloy-Z. The failure mechanism was described as stress rupture. In the present work the failure site shown for Narloy-Z in Fig. 4(b) does not show necking of the material adjacent to the crack. Therefore, the visual evidence in the present work supports the Ref. 4 contention of a tensile stress failure mechanism only with OFHC copper. The failure sites for the Narloy-Z and heat treated Amzirc in the present work are different than observed in Ref. 4 because there is no evidence of necking adjacent to the crack with these materials.

Effect of Cyclic Testing on Material Properties

Some metalographic observations were made for the material at the failure sites. It appears that some recrystalization has occurred in the hot gas wall of the OFHC copper chamber S/N 75 (Fig. 4(a)). No recrystalization was observed for the other materials. When hardness surveys were taken across sections similar to those shown in Fig. 4, it was found that hardness adjacent to the failure site was different from hardness away from the failure site (near the electroformed closeout). If it is assumed that the liner material away from the failure site remained in the pretest condition, then a change in hardness occurred at the failure site for all liner materials during cyclic testing. A tabulation at hardness measurements for each chamber are shown in Table I. The as fabricated hardness with OFHC copper was R_B 12-15. At the failure sites there was softening to R_B 0-9. In contrast the heat treated Amzirc and Narloy-Z hardened as cycles were accumulated. Heat treated Amzirc hardened from R_B 10 to R_B 15, Narloy-Z chamber S/N 140 hardened from R_B 33 to R_B 57. Narloy-Z chamber S/N 150 hardened from R_B 45 to R_B 60. An observation can be made that both Narloy-Z chambers failed at about the same hardness, but the one that hardened more (R_B 33 to 57) had longer life (301 compared to 154 cycles). The reasons for these differences in material behavior is not understood.

Effect of Materials on Deformation Rate

The hot gas side wall deformation was measured nondestructively. Polar plots were made for each of the thrust chambers to document the post test hot gas wall deformation. A typical plot is presented in Fig. 5(a). It can be seen in the figure that the failure site and one or two other channels exhibit the double bump characteristic (each cooling channel covers a 6° arc). The deformation at the failure site is much greater than at other locations in the thrust chamber. This was true for all materials. The deformation data from these polar plots are tabulated in Table I. Deformation at the failure site was defined as the distance from the valley (at approx. the rib center line) to the largest peak. The data tabulated was for the largest observed hot gas wall deformation measured from plots such as Fig. 5(a).

Since the method for measuring deformation was nondestructive, it was also employed to obtain deformation data of intermediate life points. Two variations of the nondestructive method were used. First, the 360° plots previously described could be made at various axial locations, but that required removing the chambers from the thrust stand. Second, it was found that after the most highly deformed area had been located, data could be taken from plaster costs of the area. These intermediate life data are also recorded in Table I. An example of intermediate life hot gas wall deformation data is shown in Fig. 5(b) for OFHC copper chamber S/N 74 after 124 cycles. The polar plots were made at various axial stations in the vicinity of the most highly deformed area. The potential failure site can readily be identified even though the failure did not occur for another 69 cycles. The double-bump characteristic is also evident. As can be seen from Table I there was good agreement between deformation data using the two methods for OFHC copper chamber S/N 74 at 124 cycles. The 360° plots indicated a deformation of 0.173 mm (0.0068 in.) and the plaster cast method indicated 0.155 mm (0.0061 in.).

A significant observation from the intermediate life deformation data is that the failure site was identified early in the life of the chamber. For example, with chambers S/N 75 and 82 the potential failure sites were identified prior to the mid-life point. The failure site was identified just past the mid-life point with S/N 74 (see Table I). It is likely that if data had been recorded earlier in the life of these chambers, especially the copper chambers S/N 74 and 75, the failure site could have been identified earlier.

The failure site deformation data for the two OFHC copper chambers (S/N 74 and 75) and for the heat treated Amzirc chamber (S/N 82) are presented in Fig. 6(a) as functions of accumulated cycles. Where available, data using both nondestructive methods, that is, from paster cast segments and full 360° plots are shown. The closed symbols are the post failure points and represent an average of the nondestructive and the post failure photographic data. Even as the deformation becomes large the failure site bulges out into the chamber in a nearly linear manner as cycles are accumulated. Reference 5 has characterized the failure mechanism as a ratcheting type process. The slope of the deformation histories presented in Fig. 6 could be considered a ratcheting rate. The ratcheting rate for the OFHC copper is nearly 3 times greater than the heat treated Amzirc. As noted in APPARATUS the stiffness of the structural jacket for the OFHC thrust chambers was less than the other chambers. [illegible] reported in Ref. 6 that the low stiffness structure reduced the strain range approximately 10% compared to the thick nickel structure. Consequently, if the OFHC copper chambers had been fabricated with the same stiffness the trend would be toward increasing the ratcheting rate for the OFHC copper.

A rapid increase in the hot gas wall deformation can be seen in Fig. 6(a) just before failure with the OFHC copper. At the onset of failure the material no longer ratchets linearly but becomes unstable and rapidly deforms (thins) until a tensil stress failure occurs. This was seen visually in

the cross section photograph (Fig. 4(a)) as local necking of the material adjacent to the crack. The rapid deformation and thinning may have occurred in the final cycle or progressively during the last nine cycles.

The ratchet rate curve for the heat treated Amzirc is not as well defined as the OFHC copper. A linear curve was drawn using the origin and the single mid life data point. This curve was extrapolated to 250 cycles. Since the post failure data are close to this linear ratchet rate curve the indication was that the material does not become unstable and rapidly deform at the onset of failure. As was stated earlier, the cross section photographs of the heat treated Amzirc and the Narloy-Z failure sites did not indicate local necking of the material adjacent to the crack. The post failure deformation data for the two Narloy-Z thrust chambers are shown in Fig. 6(b) along with the deformation histories for the OFHC copper and heat treated Amzirc chambers presented above. A single deformation rate curve could be used for both Narloy-Z chambers, but with failure occurring at different points.

It appears that ratcheting rate is unique for each material, and that it is nearly constant for any particular failure site. In the case of the two Narloy-Z chambers the ratcheting did not proceed for the same number of cycles before a failure occurred. The ratcheting rate data in Fig. 6 are for a specific set of operating conditions and geometry, and therefore, do not have universal application. But, if early identification of failure sites and ratcheting rate can be applied to a failure mechanism which relates to minimum wall thickness, there is the potential for estimating the remaining cycles to failure.

Correlation of Deformation with Hot Gas Wall Thinning

Figure 7 shows the final failure site deformation versus the final failure site hot gas wall thickness for three different thrust chamber materials. The data were obtained by measuring cross section photographs. The definition of deformation was the same as used with the polar plots (Fig. 5). The wall thickness was measured as indicated in Fig. 4. As shown in Fig. 7 the wall thickness versus deformation data are correlated by a straight line which extrapolates to the original wall thickness of 0.889 mm (0.035 in.) for zero deformation. Although this correlation was made from post failure data it is assumed that the correlation is also valid at intermediate life. Use of this correlation provides a means for determining wall thickness at intermediate life points from measurements of hot gas wall deformation.

For example, the use of the correlation between hot gas wall deformation and thinning made it possible to estimate the wall thickness for the OFHC copper at the onset of failure. By extrapolating the OFHC ratcheting rate curve (Fig. 6(a)) to 200 cycles it can be seen that at the onset of failure the deformation was approximately 0.25 mm (0.010 in.). From Fig. 7 it can be seen that 0.25 mm (0.010 in.) deformation corresponds to a wall thickness of 0.475 mm (0.0187 in.).

Discussion of Failure Mechanisms

As noted in Ref. 4 and as can be seen in Fig. 4(a) of the present work the visual evidence supports the contention of tensile stress failure with OFHC copper. For a tensile stress failure to occur, the ultimate stress for the material must be exceeded at some point in the cycle. The exact point in the cycle when failure occurred is not known since both the stress in the wall and the ultimate stress of the material are changing with time. The stress is nominally the same for all three materials for the same wall thickness and would increase as the wall thickness decreases. Therefore, it is assumed that a wall thickness of approximately 0.475 mm (0.0187 in.) corresponds to a stress in the wall equal to the ultimate stress value of OFHC copper. The result is a tensile stress failure. However, since the published data for heat treated Amzirc and Narloy-Z indicate that the ultimate stress is greater than OFHC copper at similar temperature conditions, the level of stress in a wall 0.475 mm (0.0187 in.) would not produce a tensile stress failure in these stronger materials. Figure 7 shows that these stronger materials possibly failed at stress levels even less than the OFHC copper since the final wall thickness was greater than with OFHC copper. The implication is that the failure mechanism for the heat treated Amzirc and Narloy-Z thrust chambers in the present work is more complicated than simple tensile stress failure.

Concluding Remarks

Analytical models attempt to predict the conditions present in typical locations. But, every real thrust chamber will have a local site that will behave atypically and as a result will eventually become the first failure site. For the thrust chambers which have been tested to cyclic failure, the failure mechanism appears to be one of accumulating deformation on a cycle-by-cycle basis (ratcheting). The fact that each chamber will have only one, or very few, failure sites can be either a disadvantage or an advantage. It is a disadvantage if it is not possible to characterize the anomalies that make a local site atypical in a way that can be included in an analytical model. Consequently, a priori life predictions could not be made. The advantage of singular failure sites is that quite possibly their appearance may not mark the end of the useful life of the thrust chamber. Testing has generally been stopped at the onset of a through crack. As a result there is only limited published information on the rate of crack growth and the rate of coolant leakage into the thrust chamber as additional cycles are accumulated. It is not known, for instance, whether the crack growth will be cyclic and/or time dependent.

Summary of Results

A test program to investigate the deformation and surface roughening of rocket thrust chambers subjected to cyclic testing was conducted. Five thrust chambers were fabricated by milling coolant channels into copper or copper alloy liners. The cooling channels for three of the chambers were completed and structural strength added by electrodepositing a thick nickel closeout onto the liner. The cooling channels for two of the chambers were completed by electrodepositing a thin layer of

copper onto the liner. Structure strength was then added to these two chambers by applying a fiberglass wrap over the metallic liner. The propellants used were gaseous hydrogen and liquid oxygen. A separate flow of liquid hydrogen was used as thrust chamber coolant. The combustion chamber pressure was 4.14 MN/m^2 (600 psia). The throat diameter was 6.60 cm (2.60 in.). The following results were obtained:

1. A ratcheting type deformation process was present when milled channel thrust chambers were tested cyclically. Ratcheting is characterized by progressive bulging of the hot gas wall into the combustion chamber accompanied by thinning of the wall at the coolant channel center line. The ratcheting continued until a crack was produced in the hot gas wall.

2. Ratcheting rate was determined for OFHC copper, Narloy-Z, and heat treated Amzirc by measuring the amount the hot gas wall deformed (bulged) at intermediate points during the life of the thrust chambers. The ratcheting rates were different for each material.

3. Ratcheting rate was nearly linear throughout the life of both OFHC copper and heat treated Amzirc chambers. The lowest ratcheting rate was with the heat treated Amzirc. Post failure data with Narloy-Z indicates a ratcheting rate between the OFHC copper and heat treated Amzirc.

4. Hot gas wall deformation was correlated with hot gas wall thinning by a single straight line for OFHC copper, Narloy-Z, and heat treated Amzirc thrust chamber liners.

5. The potential failure site could be identified near mid-life for most chambers using nondestructive methods to monitor deformation of the hot gas side surface.

6. The failure mechanism observed with the two OFHC copper thrust chambers in the present work was consistent with the stress rupture type mechanism described in Ref. 4. But, the failure mechanism with the heat treated Amzirc and Narloy-Z thrust chambers in the present work was more complicated than simple tensile stress failure.

7. OFHC copper strain softened, and Narloy-Z and heat treated Amzirc strain hardened as cycles were accumulated.

References

1. Fulton, D., "Investigation of Thermal Fatigue in Non-Tubular Regeneratively Cooled Thrust Chambers, Vol. 1," Rockwell International Corp., Canoga Park, Calif., R-9093-Vol. 1, May 1973. (AD-760582; AFRPL-TR-73-10-Vol. 1.)

2. Fulton, D.: "Investigation of Thermal Fatigue in Non-Tubular Regeneratively Cooled Thrust Chambers, Vol. 2," Rockwell International Corp., Canoga Park, Calif., R-9093-Vol. 2, May 1973. (AD-760583; AFRPL-TR-73-10-Vol. 2.)

3. Andrews, J. S. and Armstrong, W. H., "The 3.3 K Thrust Chamber Life Prediction," Boeing Aerospace Co., Seattle, Wash., D180-18170-1, Aug. 1974. (NASA CR-144048)

4. Quentmeyer, R. J., "Experimental Fatigue Life Investigation of Cylindrical Thrust Chambers," AIAA Paper 77-893, July 1977. (NASA TM X-73665, 1977.)

5. Hannum, N. P., Kasper, H. J., and Pavli, A. J., "Experimental and Theoretical Investigation of Fatigue Life in Reusable Rocket Thrust Chambers," AIAA Paper 76-685, July 1976. (NASA TM X-73413, 1976.)

6. Kasper, H. J. and Notardonato, J. J., "Investigation of the Effect of Low Stiffness Closeout on Rocket Thrust Chamber Life," NASA TP-1979.

7. Quentmeyer, R. J., Kasper, H. J., and Kazaroff, J. M., "Investigation of the Effect of Ceramic Coatings on Rocket Thrust Chamber Life," AIAA Paper 78-1034, July 1978. (NASA TM-78892, 1978.)

8. Pritz, W., George, D., and Evans, S. A., "The JANNAF Rocket Engine Performance Prediction and Evaluation Manual," Chemical Propulsion Information Agency, John Hopkins U., Baltimore, Md., CPIA Publ-246, Apr. 1975.

TABLE I

Material	S/N	Failure site deformation				Failure site wall thickness		Accumulated cycles	Material hardness	
		Polar plot		Pictures					As fabricated	Failure site
		mm	in.	mm	in.	mm	in.		R_B	R_B
Narloy-Z	140	0.196	0.0077	0.196	0.0077	0.592	0.0233	[b]301	33	57
	150	.135	.0053	.135	.0055	.650	.0256	[b]154	45	60
Heat Treated Amzirc	82	.030	.0012	-----	------	-----	------	99		
		.135	.0053	.089	.0035	.711	.028	[b,c]250	10	15
OFHC Copper	74	.160	.0063	-----	------	-----	------	114		
		.173	.0068	-----	------	-----	------	124		
		.155	.0061	-----	------	-----	------	[a]124		
		.183	.0072	-----	------	-----	------	[a]154		
		.216	.0085	-----	------	-----	------	[a]184		
		.404	.0159	.399	.0157	.290	.0114	[b]193	15	9
OFHC Copper	75	.091	.0036	-----	------	-----	------	94		
		.361	.0142	.356	.0140	.277	.0109	[b]202	12	<0

[a]Data from plaster cast.
[b]Post failure data.
[c]Cycles to failure uncertain.

(a) COMPLETED FATIGUE CHAMBER.

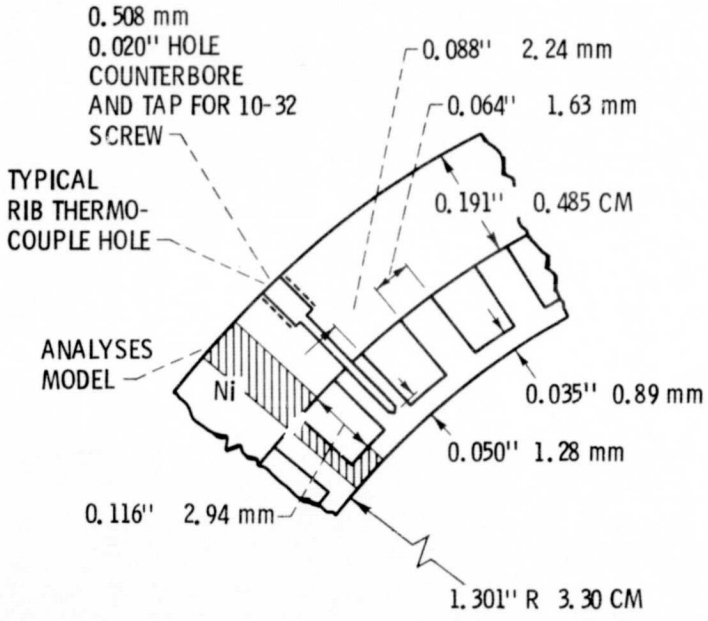

(b) WALL CROSS SECTION AT THE NOZZLE THROAT.

Figure 1. - Fatigue combustion chambers.

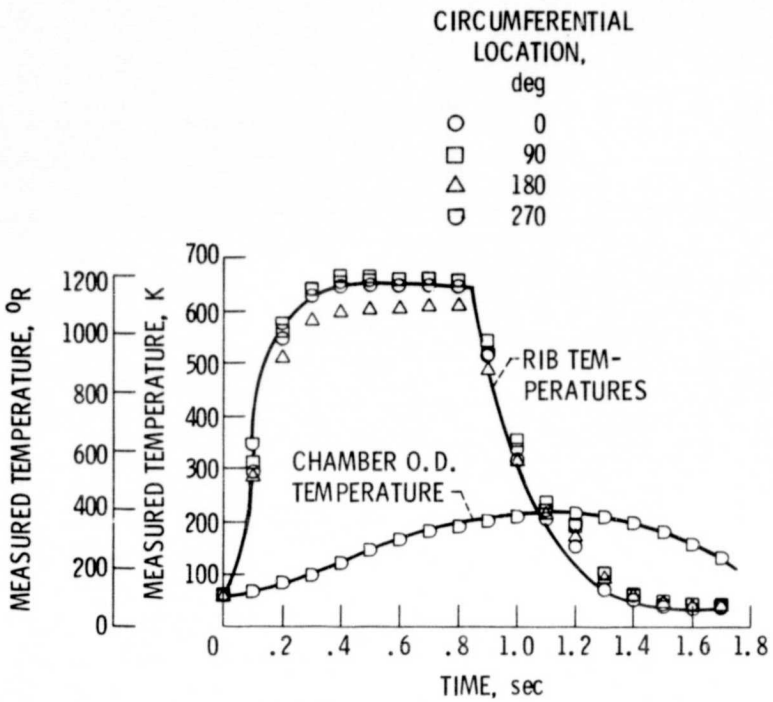

Figure 2. - Measured rib temperatures and chamber O.D. temperature as function of time for one firing cycle. Chamber S/N 70.

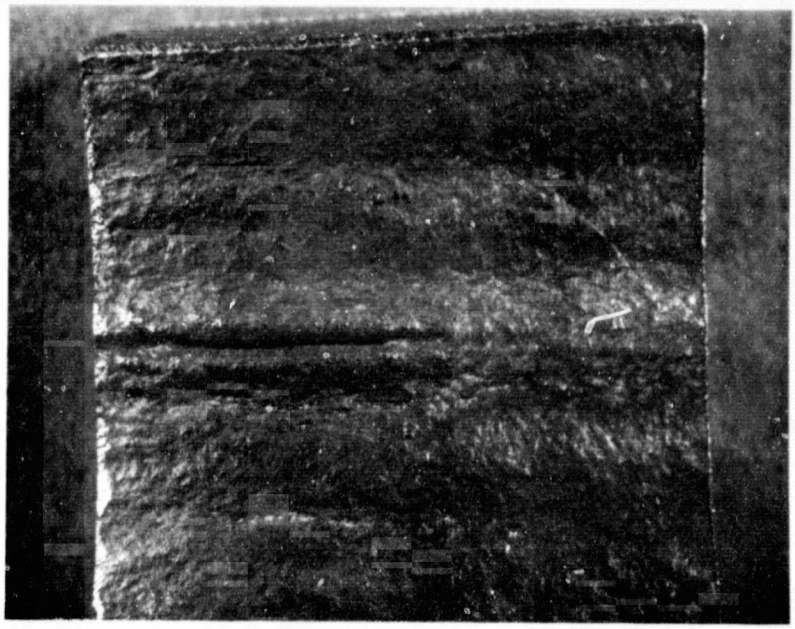

(a) VIEW OF THE HOT GAS WALL SHOWING A TYPICAL CRACK THROUGH THE WALL JUST UPSTREAM OF THE THROAT.

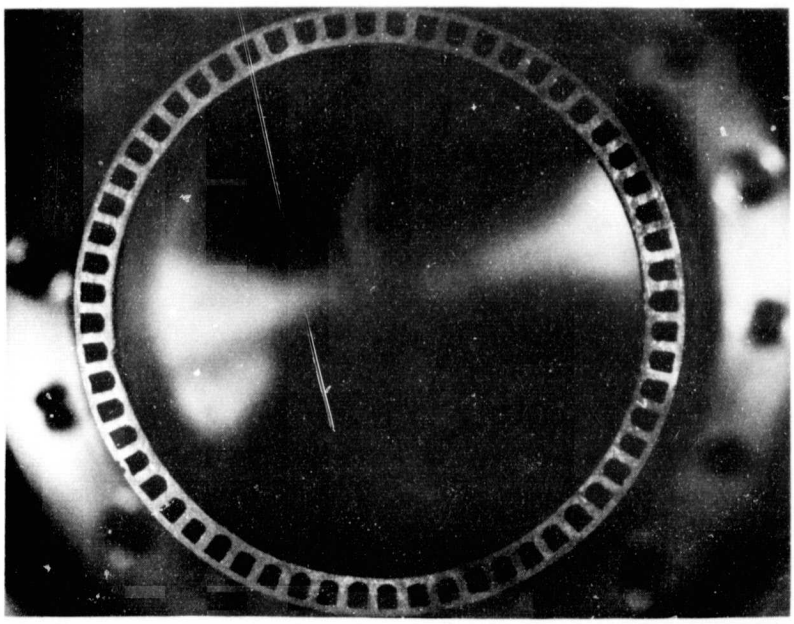

(b) CROSS SECTIONAL VIEW TAKEN IN THE THROAT PLANE SHOWING THE 60 COOLING CHANNELS AND THE ELECTROFORMED CLOSEOUT.

Figure 3. - Photographs of OFHC copper thrust chamber S/N 74 typifying the failure site and deformation of the hot gas wall.

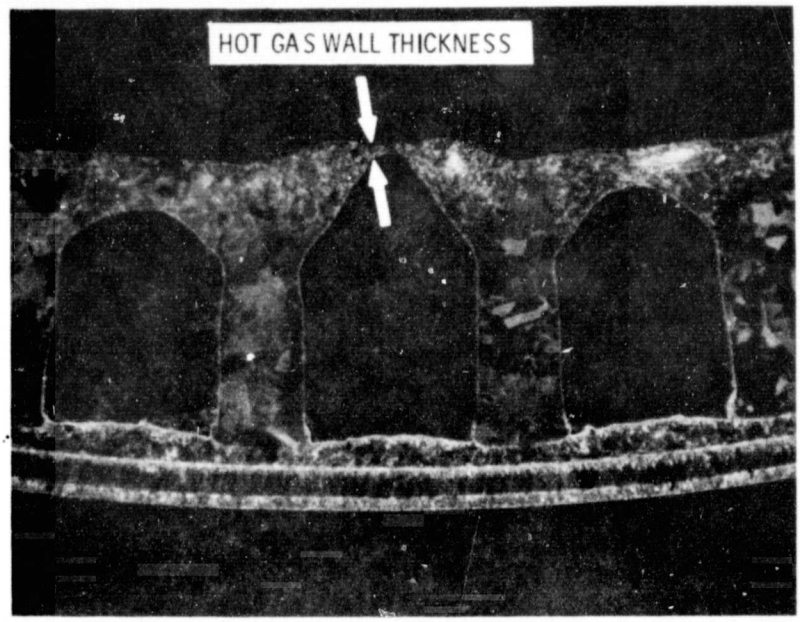

(a) OFHC COPPER THRUST CHAMBER S/N 75.

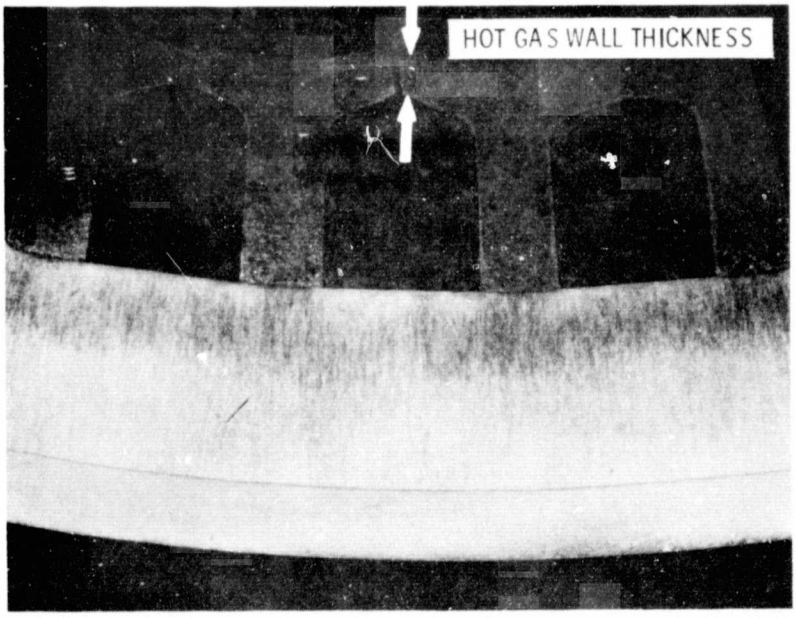

(b) NARLOY-Z THRUST CHAMBER S/N 150.

Figure 4. - Cross sectional view of failure sites.

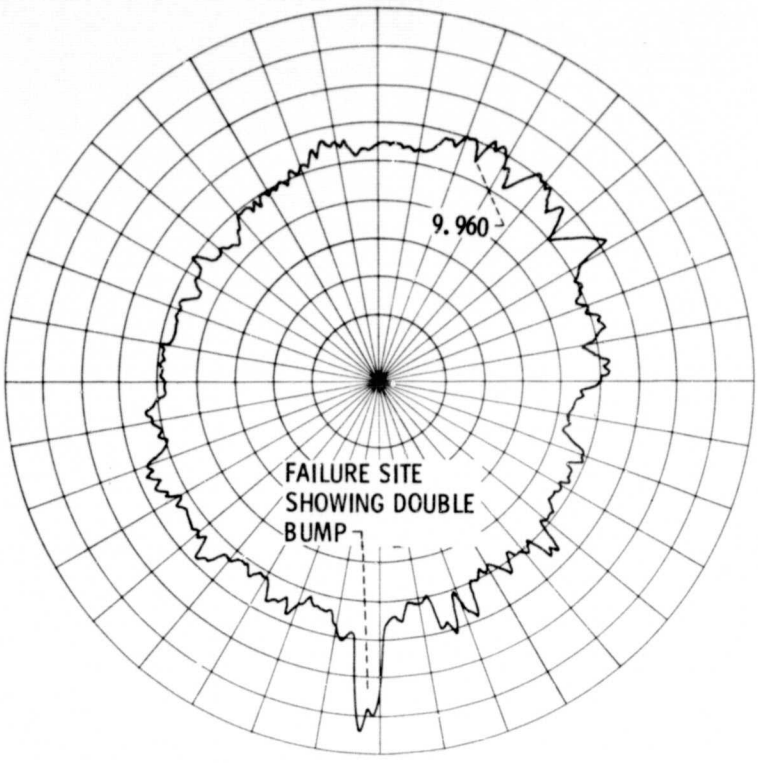

(a) POST FAILURE DATA AFTER 193 CYCLES.

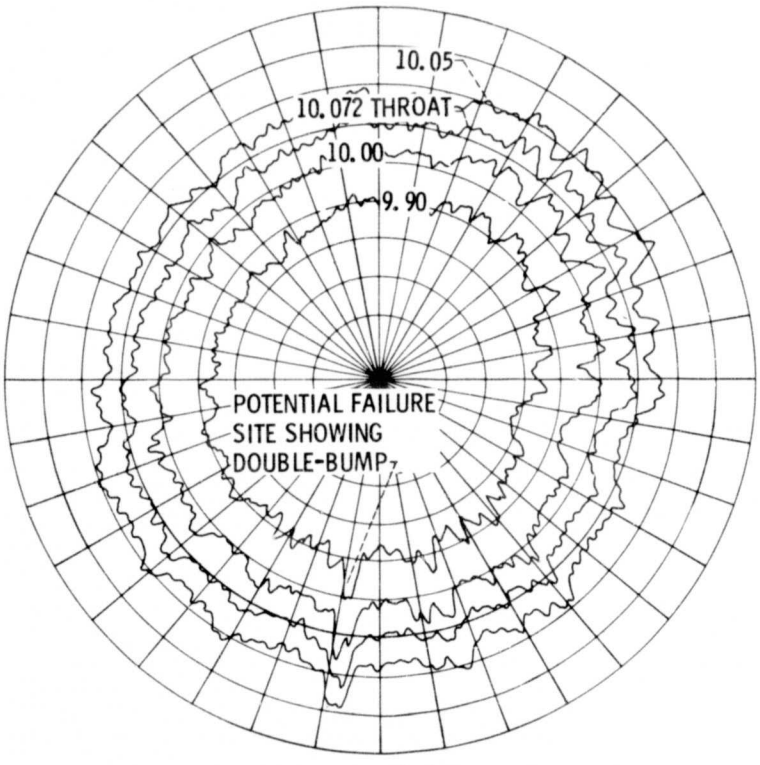

(b) INTERMEDIATE LIFE DATA AFTER 124 CYCLES.

Figure 5. - Polar plots of OFHC copper chamber S/N 74 showing hot gas wall deformation.

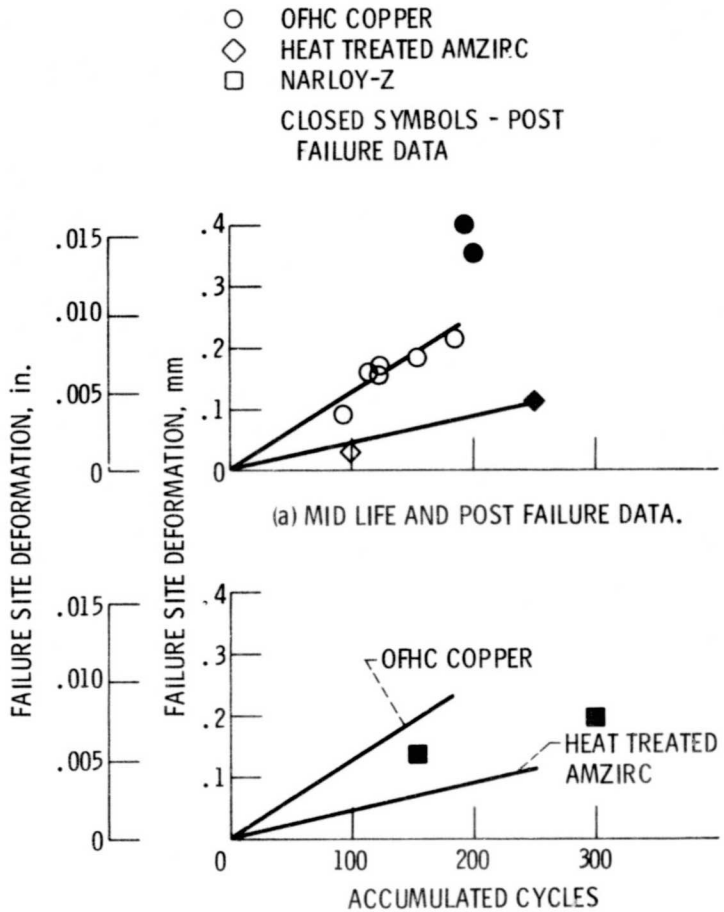

Figure 6. - Failure site deformation as a function of accumulated cycles.

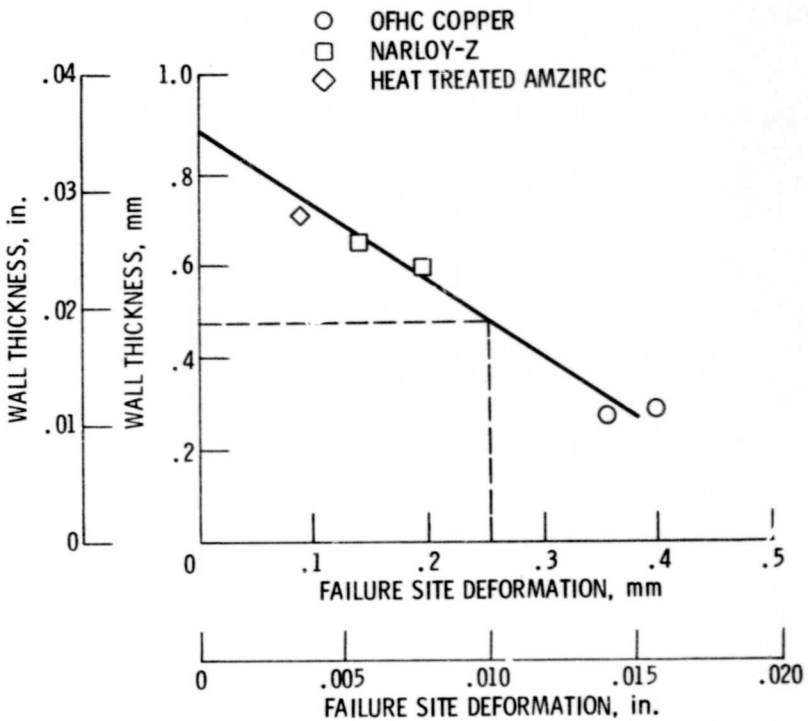

Figure 7. - Relationship of failure site deformation to coolant channel wall thickness for three different thrust chamber liner materials.